

Expert Opinion

1. Introduction
2. Nano-scale characterization methods
3. MRI
4. PET and SPECT (radio isotopic imaging method)
5. Electron paramagnetic resonance imaging
6. Optical imaging methods
7. Hybrid imaging
8. Expert opinion

A review of imaging methods for measuring drug release at nanometre scale: a case for drug delivery systems

Ketan Pancholi

The Robert Gordon University, School of Engineering, Aberdeenshire, UK

Introduction: Current drug delivery research is focused on improving the efficacy of drug delivery systems, with emphasis on precise targeting, accurate dose delivery, strategies for overcoming the tissue barrier and monitoring the effects of drugs on their targets. To realize these goals, it is essential to determine the spatio-temporal bio-distribution of particles in the whole animal. Enabling such a measurement at the nanometer scale helps in the design of efficient systems.

Areas covered: This article discusses the need for molecular imaging in drug delivery development and also reviews promising imaging methods. Moreover, the physics behind each method is explained and evaluated to derive advantages and limitations. The review enables the readers to select, use and modify the existing methods to implement imaging protocols for studying drug release from particular drug delivery.

Expert opinion: Currently, the difference in pharmacodynamics obtained via various imaging modalities cannot be verified and hinders clinical use. To establish imaging as a scientific tool, its translation into clinical use is vital. Presently, there is no single imaging method suitable for drug-release studies. However, hybrid imaging has the potential to provide the desired imaging system.

Keywords: diffusion measurement, drug delivery, drug diffusion, drug-release quantification, drug-release study, imaging, molecular imaging, nano-scale characterization

Expert Opin. Drug Deliv. (2012) (2):203-218

1. Introduction

The primary aim of the drug delivery system (DDS) is to deliver the drug to the target with high precision and control. Nano-particles as drug carriers do not leak rapidly through vasculature and also avoid entrapment by the fixed macrophage due to their unique size. Additionally, their stable structure provides longer shelf life and retention in blood circulations. Many systems have demonstrated the targeted control release using polymer nano-particles and liposomal platform [1-6]. To refine such control further, properties affecting diffusion can be manipulated. Hence, micro-managing polymer-drug conjugation [7,8], physical properties [9,10], physiological microenvironment [11,12] and drug-release mechanism [13] is crucial. For example, salt-gelatine complex in contact lenses alters the physical property of gelatine and controls the release of active ingredient in the eye [14]. With advances in genomics and proteomics, new drug molecules with complex physiochemical properties are emerging rapidly. To deliver such drugs with poor solubility, short half-lives, vulnerability to degradation, low permeability and molecular size, a significant understanding release mechanism is required [15]. Many approaches such as the addition of a modifying agent, [16] sonoporation [17], electroporation [18], polymer-drug conjugation [19,20] and the use of a variety of drug carriers [21,22] have been utilized to deliver complex

informa
healthcare

Article highlights.

- When nano-scale imaging is combined with genomics, it creates a perfect tool for biology interrogation at the system level and, thus, makes it crucial for drug delivery research.
- An ideal imaging system should detect a pharmacologically relevant drug concentration in whole animal with high spatial, temporal and depth resolution.
- All methods are classified according to their use in imaging drug release in whole body or at cell level.
- Imaging of drug release at nano-scale enables visualization of subcellular processes and relates them to tissue changes and drug dosages in clinical set up.
- Imaging can visualize the dismissal of any biological pathways, tolerances in live biological network during fast quantitative data acquisition to facilitate identifying the drug delivery system with unfavorable pharmacokinetics and toxicity at an early stage of clinical trials.

This box summarizes key points contained in the article.

molecules [23,24]. However, in absence of a method capable of measuring the release as a function of applied stimuli, release rate obtained in laboratory is difficult to be replicated *in vivo* [25,26]. Hence, efficient characterization techniques to measure drug release in relation to physiological environment, formulation of particles and its physical properties are required to enable an efficient design [27].

1.1 Requirement of nano-scale information

A drug-release study consists of measuring drug concentration in releasing media as a function of time. First, drug infused particles are dispersed in constantly stirring simulated body fluid. At regular intervals, a small amount of fluid is extracted to determine concentration using methods such as NMR [28,29], dye tracing [30,31], spectroscopy [32] and liquid chromatography [33]. Although it provides crucial information, knowing the amount of drug that has reached the target, the effect it has on the target and the effect of the stimuli/physical properties on release is essential [34,35]. Moreover, observing interaction between solvent and carriers or enteric coating develops crucial insight for designing [36,37].

At nano-scale, release behavior can be correlated to intrinsic structure and materials of particles. Moreover, assessment of target realization, barrier negotiation and residence time is also possible [38,39]. For example, optical imaging established the fact that the nano-particles of 100 nm diameter can circulate in body for longer period but their negative surface charge enhances the particle convection through matrix repulsion [40]. Similarly, nano-scale atomic-force and confocal microscope images of lipoplex-cell interaction helped determining charge ratio required for internalization through membrane.

Studies such as cytotoxicity, ligand-receptor and drug-cell interaction can only be observed at molecular level. Recently, nano-scale imaging helped in identifying the role of precursor present on surface of gold nanorods in their cytotoxic

behavior [41]. Similarly, molecular specificity enables visualization of subcellular processes and relates them to tissue changes and drug dosages in clinical set up. Endogenous or exogenous contrast agent can be functionalized to attach to target to express signaling pathways changes in the presence of enzyme. Determining expression at target detects disease and measures therapeutic concentration allowing determining delivery trigger. High resolution can confirm inhibition and activation of specific target function. For example, molecular image of satin treated rodent aorta showed the low uptake of vascular cell adhesion molecule internalizing iron oxide particles [42].

2. Nano-scale characterization methods

Nano-scale characterization are divided into imaging and non-imaging methods. Imaging records data in 2D or 3D format while non-imaging methods acquires it in one dimension. Multidimensional data permit analysis using registration, segmentation and image correlation. An image segmentation followed by registration identifies volume of interest and aligns it to the subject area. This determines the spatial position of carriers on an organ plane while autocorrelation of images calculates diffusion coefficient at nano-scale [43-45].

2.1 Non-imaging methods

Although these methods involve histopathological analysis of the collected blood and tissue [46,47], it has not yet been fully substituted by any other techniques. Because of its easy availability, low cost and clinically approved status, it has been regularly used in clinical set up. For example, non-imaging methods such as tape stripping, microdialysis, skin biopsy, suction blister and follicle delivery are still in use to determine topical availability of the drug [48-53]. Development in proteomics and genomics has added another capability of detecting target expression capable of indicating disease and therapy response. Similarly, metabonomics procedures provided biomarkers for drug efficacy or toxicology tests [54].

2.2 Imaging methods

These methods can help replacing, reducing and refining the use of small animal imaging in drug-release studies. Using contrast agent, imaging can visualize the dismissal of any biological pathways, tolerances in live biological network during fast quantitative data acquisition [55,56]. Correlating these data to particle size and porosity [57] facilitates recognizing DDS with unfavorable pharmacokinetic and toxicity at an early stage of clinical trials [58]. However, this information cannot be used as a substitute for clinical trials [59].

Each imaging modality should be selected on its merits. For instance, γ -scintigraphy or positron emission tomography (PET) can assess DDS efficacy in humans due to its unlimited depth resolution [60] but exposes to ionizing radiation [61,62]. High resolution FTIR captures polymer phase development, the polymer-solvent interface speed and polymer chain relaxation in nano-particles [63,64] while high depth resolution

of MRI and sonography enable probing adhesive property of drug carriers [65,66]. In contrast, optical methods have high spatial and temporal resolution but low depth resolution [67].

Ideal imaging system should detect pharmacologically relevant drug concentration in whole animal with high spatial, temporal and depth resolution. The signal to noise ratio (SNR) must be high enough to identify drug molecule in tissue background. In this article, all methods are classified according to their ability to image in whole body or at cell level. A summary of advantages and disadvantage is provided in Table 1 while their clinical use is listed in Table 2.

3. MRI

This method works on the principle of magnetic resonance. When magnetic field-induced alignment of atom nuclei is disturbed by the radio pulse, the weak magnetic field is generated, which subsequently induces voltage in surrounding coil forming signals. The degree of influence by neighboring atom determines the time taken by magnetic dipole to come to its baseline from an excited state. Such time, termed as 'relaxation time,' is different for the same molecule present in a different physio-chemical environment. For example, relaxation time of hydrogen nuclei will be different in a carbon rich environment than in water. This allows imaging at greater depth with excellent soft tissue contrast [68,69].

High contrast between water and polymer allows identifying domains with varying degree of hydration in drug carriers. Such identification is enabled by determining spatial distribution of T_2 signals using spin echo and diffusion weighted imaging [70]. In pharmacokinetic context, decreasing T_1 (spin-lattice interaction) and T_2 (spin-spin interaction) amplitude facilitates high contrast images whereas intensity and position of resonance frequency identify the molecules. Attaching $MnSO_4$ [71] and gadolinium [72] to the molecules, the contrast can be improved via T_1 shortening.

3.1 Whole body study

For whole body imaging, a contrast agent is required. For instance, doping liposomes with $MnSO_4$, the influence of temperature on uptake and bio-distribution of liposome in rat was measured. In this experiment, first, rat was immobilized to administer liposome dose. Target site temperature was regulated by running $MnSO_4$ doped hot water through inserted catheter before imaging. Resultant images detected accumulation of thermally sensitive liposomes at the target and thermally insensitive liposomes at periphery [73]. Alternatively, high magnetic field and dedicated hardware are used to enhance contrast [74]. MRI has detected the difference between *in vitro* and *in vivo* release of gadolinium chelated Gd-DTPA episcleral implant. Images showed that the implant failed to deliver drug to

posterior segment of eye as was observed in laboratory results [75].

3.2 Cell level study

Tissue factor targeted nano-particle uptake by cell was accurately quantified via measuring difference between T_1 before and after administrating particles. Particle carrying 94,000 gadolinium chelates produced relaxivities relative to the nano-particle concentration of $910,000 (s \cdot mM)^{-1}$ at 4.7T. This enables a minimum detection limit to generate an SNR of 5 for 113 pM concentration. Clear images were obtained at low nano-particle concentration (occupied < 1% volume of the total number of voxel) [76].

4. PET and SPECT (radio isotopic imaging method)

It is considered as the most clinically relevant method due to its unlimited depth resolution. Its radioactive probes such as ^{11}C , ^{15}O , ^{18}F and ^{13}N generate high energy signal (two photons of 511 kV) that are detected by the circularly arranged scintigraphic sensors to construct 3D volume images. Each pixel represents the concentration and position of the radionuclide on the scanning plane of the organ. However, linear correlation between drug concentration and pixel intensity exists in PET images whereas it does not exist in single photon emission CT (SPECT) images due to variable photon attenuation values [77].

Each method acquires images in different ways. PET uses events measured from all angles and linear positions to construct images whereas SPECT uses γ -rays coming from linear positions only. Because SPECT blocks signals emitted at angles, its signals are weaker in comparison to PET. However, the sensitivity of such signals can be improved using pinhole collimator with a short focal length [78,79]. A typical sensitivity of SPECT is limited to 10^{-9} mol/l whereas PET can detect the drug with a sensitivity of 10^{-12} mol/l [80].

4.1 Whole body study

Fast release in whole body is captured using short-life radionuclides (PET) whereas long-life radionuclides are used for slow release. For example, SPECT imaging requires highly sensitive radio iodine labeled antibody (^{125}I -833c) to determine antibody targeting to the thoracic cavity and its colocalization with a perfusion marker [81]. The spatio-temporal distribution of antibodies and its kinetic data verified the uptake by lungs, which otherwise declined by first-order kinetics.

Receptor-specific ligand can be labeled to detect the barrier negotiating capability of the drug. In a representative experiment, SPECT equipped with pinhole collimator was used to obtain dynamic images of radio-labeled dopamine transporter in rat [82,83]. Pin-hole collimation increases resolution and reduces the partial volume error but PET requires an image-reconstruction algorithm for

Table 1. Comparison of imaging modalities for drug delivery characterization.

Method	Ionizing	Depth penetration	Sensitivity	Advantages	Disadvantages
Electronic paramagnetic resonance	No	Small animal capability	Sensitive to low concentration	Non-invasive method, ability to sensitively image heterogeneous and solid samples with high degree of specificity	Requirement of the addition of paramagnetic material and the size restrictions for the <i>in vivo</i> measurements
MRI/magnetic resonance spectroscopy	No	No limit	Limited at low concentration	Non-invasive method, pharmacologically relevant drug concentration detecting ability, high tissue contrast	Only functional exogenous agent can be followed, relatively low temporal resolution, variability in colocalization of drug and contrast agent, large voxel size
PET/SPECT	Yes	No limit	High sensitivity at low concentration	Good temporal resolution (many images/min), high sensitivity, able to detect early molecular event	Low spatial resolution, need radiolabel, cannot detect physical changes in drug carrier during drug release, detects one molecular event per scan
CT	Yes	No limit	High sensitivity at low concentration	Excellent spatial resolution	Requires contrast agent, temporal resolution inferior to PET/MRI, cannot detect physical changes in drug carrier during drug release
Raman microscopy (CARS/SRS)	No	Small animal	High sensitivity at low concentration	Higher spatial resolution, non-invasive and label-free high chemical contrast imaging, sensitive to low concentration	Strong background signals and hence low detection sensitivity, low temporal resolution, relatively flat surface is required
Thermoacoustic/photo-acoustics	No	Limited < 1 mm at high resolution and 10 cm at low resolution	High sensitivity at low concentration	High spatial resolution, excellent chemical contrast, non-invasive, safe, ability to image at greater depth than Raman spectroscopy, less background noise	Mathematical model dependency, depth profiling is complicated, contrast agent needed for drug-release study, radio frequency induced thermoacoustic imaging yield depth resolution of 10 cm
Ion spectroscopy	No	Limited	Limited at very low concentration	High sensitivity, submicrometer resolution, provides structural and molecular information simultaneously, capable of detecting small to large fragile molecules	Comparative low chemical contrast, complex sample preparation, possible degradation of samples due to high voltages, strong interaction with background signals in bio samples, smart matrices are needed, excellent <i>in vitro</i> applications
MXF	Yes	Small animal	High sensitivity at low concentration	Good chemical contrast, better depth penetration than optical methods, no need of flat surfaces, non-invasive	Low resolution (5 – 10 μm), low temporal resolution, can be applied as a micro focus computer tomography, use of phase contrast approach requires lower X-ray fluence for <i>in vivo</i> imaging

CARS: Coherent anti-stoke Raman spectroscopy; PET: Positron emission tomography; SPECT: Single photon emission CT.

reducing the error [84]. Use of receptor-specific tracers such as dopamine ligands increases specificity and helps measuring receptor occupancy [85]. Specific ligand enhances the capability of SPECT to enable studying psychotic and depressive diseases.

4.2 Cell level study

Measuring amount of radiation in a cell can determine bio-distribution of nano-particles. In one such example, animal organ was sectioned after administering radio-labeled nano-particles. Subsequently, PET images were acquired depicting

Table 2. List of imaging methods and their suitability for detecting particular diseases.

S. no.	Imaging modalities	Suitable clinical application
1	MRI/magnetic resonance spectroscopy	Neurological disease, CNS disease, various metabolic disorder, musculoskeletal
2	Optical imaging (OCT) endoscope	Bladder, esophagus, digestive system
3	Optical imaging (OCT)	Periodontal disease, eye disease, skin
4	Optical imaging (multiphoton microscopy)	Skin disease
5	Raman and coherence Raman spectroscopy endoscope	Atherosclerosis, breast, colonic examination
6	Coherence Raman spectroscopy endoscope	CNS, brain
7	SPECT/PET	Clinical trial modality for drug testing, inflammation, ischemic heart disease and some neurologic disorders
8	CT	Musculoskeletal, bone structure and soft tissue anatomy, inflammation, infection, perianal, pelvis area

OCT: Optical coherence tomography; PET: Positron emission tomography; SPECT: Single photon emission CT.

variation in intensity. Because intensity is proportional to the number of particles, the particle counts and drug concentration were determined. Applying micro-PET with 8 mm³ resolution reduces the partial volume error [78,86].

5. Electron paramagnetic resonance imaging

It also uses magnetic field to form the imaging signals. However, signals are formed due to resonance in electronic spin rather than nuclear spin. To generate such signals, the metal oxide molecules having unpaired electrons in its outermost shell must be attached to drug carrier. When unpaired electrons align against the magnetic field, they resonate to affect transition to a higher energy state. Amplitude of energy released as a result of reverse transition depends on the presence of number of molecules. Such variation in amplitude represents the variability in nitroxide concentration and, thus, that of drug carrier [87].

5.1 Whole body imaging

This method is constrained by low penetration of its excitation waves. Excitation frequencies in the range of 1 – 10 GHz are absorbed strongly by water rich biological samples and, thus, limit their penetration to 1 mm maximum. However, researchers measured the triaryl methyl (TAM) radical release from the subcutaneous polymer implant in live rat (~ 25 g) using lower frequency. ROI in rat body must be placed near to resonator to compensate for low sensitivity caused by low frequency. Afterwards, images were obtained and analyzed for spatial intensity profile. Because TAM release is an erosion-led process, the pixel intensity is proportional to the TAM concentration. However, it is not true for diffusion-led release process as water penetration alters the charge of nitroxide molecules to yield different spectrum shape. Longitudinally detected electron paramagnetic resonance (EPR) was used to reduce physiological movement-induced artefacts [88]. Molecular resolution of EPR is evident in an investigation on integrity of liposomes (multilayered)

during circulation in the mice [89]. Using nitroxide attached liposomes sustained release from liposomes at injection site was detected. The difference between spectral shape of encapsulated and released probe permitted their identification.

Additionally, it can also measure the drug release in relation to pH, microviscosity and other properties of microenvironment. For example, EPR proved that the polymer hydrolysis during subcutaneous poly(lactic-co-glycolic acid) (PLGA) implant degradation may decrease the pH value of microenvironment to 2. The split in nitroxide spectrum (hyperfine splitting) occurred due to interaction between unpaired electrons and magnetic nuclei of surrounding molecules indicate the pH value. When hydrolysis causes increase in polarity around implant, it increases hyperfine splitting constant and, thus, allows pH measurement [90].

Additionally, nitroxide molecule made from isotopes of nitrogen assists in multiplex imaging. However, development of pulse magnetic field gradient is required for acquiring full spectral resolution [91].

5.2 Cell level study

At cellular level, skin penetration of two compounds estradiol and procaine has been examined. In time lapsed study, the disappearance of the estradiol peak in spectrum confirmed the high penetration whereas the nearly constant height of procaine peak revealed its non-skin permeability. However, after applying procaine absorption enhancer, the observation of decrease in width and increase in height of spectrum line indicated the fluidization of the skin [92].

6. Optical imaging methods

Optical imaging is vital in drug delivery research because of its high specificity, fast acquisition rate, cheap portable set up, minimal invasiveness and high safety. Photons in optical waves relate to corresponding molecular energy level. Applying varying

energy of photons in imaging yields range of spatial and depth resolutions. For instance, white light used in compound microscope can reveal detailed drug-release mechanism in swellable polymer tablet [93] whereas pulsed laser in confocal microscope enables imaging at nano-scale. However, the improving depth resolution remains a challenge. Many indirect approaches such as application of external stimuli (plane illumination, focusing of acoustic energy), use of quantum excitation (contrast agent) and use of secondary signals (second harmonic nonlinear microscopy) have been used to yield improvement [94].

6.1 Multiphoton fluorescent microscopy

This microscopy can monitor direct drug release, subcellular processes and drug-cell interaction deep inside tissues and organs. Depth resolution from 10 μm to ~ 1 mm in some tissues, such as brain, is achieved using nonlinear light-matter interaction [95]. Nonlinear interaction occurs when many photons are simultaneously absorbed by same molecules to emit photon of twice the quantum energy. Emitted photon forms the infrared waves capable of penetrating deeper in the tissue [96]. It also enables the excitation of the UV-absorption bands of fluorophores and second harmonic generation of layered biological structures such as muscle fiber and collagen.

6.1.1 Whole body study

Images of nano-particle movement in the collagen, muscle fibers and liver tissue is dominated by the auto-fluorescence of tissue. However, using second harmonic imaging, researchers avoided auto-fluorescence to prove multistage particle's ability to travel deeper in collagen matrix [97].

Selecting fluorescent dyes is an important strategy for successful drug-release imaging. Simple fluorescent dye such as indocyanine green is selected to visualize target tissue in a clinical set up whereas synthetic fluorophores such as cyanine, chromophores, fluorescein and rhodamine can be modified for longer circulation and bioconjugation. For instance, fluorescein was metabolized for longer uptake and successful imaging of drug clearance in bile. Metabolized product mono-fluorescein glucuronide suppressed the auto-fluorescence to obtain clear images [98]. In another study, bioconjugation of Cy-5 with cyclic RGD (arginine-glycine-aspartate) improved the uptake in extra cellular matrix such that the expression of $\alpha_v\beta_3$ integrin with high specificity was detected. The study involves injecting mouse with Cy-5 labeled cRGD peptides. The images of illuminated (633 nm light) mouse body were captured using charge coupled device (CCD) (100 μs exposure time). Results demonstrated high specificity by detecting 15 times higher intensity in target tissue compared to intensity of distant skin image. It showed that the optical method can be used as a semi-quantitative, rapid, pre-PET imaging modality.

6.1.2 Cell level study

In a similar study, the probe containing buffer solution was dispersed at 37°C on the cell line 5 min before capturing

imaging. Multiphoton microscopy image of fixated cell lines captured the nano-scale details such as receptor bonding and internalization of the probe in cytoplasm confirming the ability to deliver drug intracellularly.

For a deeper and multiplex detection, quantum dots are used due to their high absorbance, two-photon cross-section, photobleaching resistance and narrow emission spectrum [99]. Use of non-hazardous green-fluorescent and luciferase protein enhances contrast as it eliminates background tissue luminescence and increases high specificity [100].

Still, it suffers from an insufficient depth resolution in dense organs including lymph node, skin, fibrous muscle and kidney. Increasing laser power induces damage to sensitive tissue without significantly increasing photon emission. Moreover, fluorescent molecule attachment may cause poor visualization of the penetration pathways [101]. Bio-inert green fluorescent protein has reduced such an effect [102] but a probe-free method is required.

6.2 Optical coherence tomography

A spatial (1 – 10 μm) and depth resolution (1 – 2 mm) of this technique places it between high spatial resolution multiphoton microscopy and high depth resolution MRI and PET imaging. It is routinely used for dermatological diagnosis due to its high SNR (130 dB) [103].

This method, analogous to the sonography, measures wave reflection (echo) at a different time to create the image. First, broadband laser beam is split into reference and sample beam using interferometer. One beam is focused on to the sample whereas the other is focused on mirror. On returning both signals are combined on photo detector. The intensity and delay of sample signal are obtained by scanning the reference mirror and measuring the interferometer. Correlating delay of the reflection beam to interferometric signal renders a clearer image. Low coherence causes signals to fall-off due to slight mismatch in delay allowing determining longitudinal position at high resolution. Because length of coherence for light source is the only limiting factor, the high depth resolution can be maintained despite small aperture [104,105].

6.2.1 Whole body imaging

This method has successfully measured diffusion of the drug and other molecules into skin, aorta, sclera and corneal tissue [106,107]. However, the surface morphology and transparency of tissue affect the results at varying degree. Unlike multiphoton microscopy, optical coherence tomography (OCT) can image a larger area with good spatial resolution. Moreover, greater depth resolution without using exogenous contrast agent can be achieved.

Its low chemical specificity restricts direct measurement of drug release. For instance, protein release from PLGA microsphere can be determined by correlating it to *in vivo* degradation of microsphere. The temporal changes in surface morphology were imaged in both conditions (*in vitro* and *in vivo*). Careful image registration identified temporal changes in morphology which, then, were correlated to find

out any difference between *in vitro* and *in vivo* release profile. Slower acquisition rate enables detecting a minimum concentration of 10^{-10} mol/l [108].

Using OCT endoscope, the detailed images of internal organ can be obtained. Researchers used the 1 mm diameter endoscope to obtain cross-section images (10 μ m resolution) of rabbit's gastrointestinal and respiratory track. The endoscope consisted of light source and time delay scanner attached to interferometer. Echo delay from scattered light was measured by interferometer to correct the spatial position. Images constructed via scanning the beam position on tissue showed the rabbit's entire esophagus while revealing high resolution details such as esophageal wall and vasculature [109].

6.2.2 Cellular study

Gold nano-particles were used to determine the effect of perforation and ultrasound radiation on internalization of nano-particles in hamster cheek pouch. The study involves imaging gold colloid treated tissue after exposing it to ultrasound (1 MHz, 0.3 W/cm²). Image of the area treated with micro-needle and ultrasound showed 177% increase in intensity confirming higher uptake of nano-particle [110].

6.3 Optoacoustic imaging

Optoacoustic imaging forms images using acoustic waves produced during absorption of ultra-short laser pulses. Local absorption in tissue causes its thermoelastic expansion. On contraction, it emits the ultrasound signals having magnitude proportional to the deposited optical energy. Because such deposition is dependent on the absorption coefficients of the absorbing agents, concentrations of these agents can be quantified via varying the wavelength [111].

6.3.1 Whole body imaging

Although deoxyhemoglobin, oxyhemoglobin and melanin in tissue act as primary optical absorbing agents, the method remains sensitive to total hemoglobin enabling acquisition of high resolution images of subcutaneous vasculature. *In vivo* imaging of the affected area of rat skin showed the higher density microvasculature in comparison to healthy tissue. Multi-spectral approach is essential for recognizing the probe attached to drug in presence of physiologically-specific tissue chromophores. For instance, highly sensitive indocyanine green dye encapsulated double emulsion was used to differentiate dye spectra from signals emanating from blood. However, reporters with high molecular specificity and sophisticated spectral processing will be required to obtain a clear signal [112].

Quantification of the drug attached to probe in tissue volume is not simple due to use of back projection algorithm, inefficient illumination detection model and nonlinear relation between sensitivity and depth. Using filtered back-projection and multispectral processing, researchers were able to determine fluorochrome Alexa fluor 750 concentrations in the small animal. To correct the photo-acoustic (PA) signal distribution, they used the mathematical model [113,114]. The

model is inverted and fitted to the known absorption value to reconstruct intensity values at each pixel depicting dye concentration. Because of its absorption spectra drops within narrow spectral window of 750 – 790 nm, PA signals were distinguished from background noise to detect 25 fmol per unit volume. It is noteworthy that the acoustic wavelength of signals must be shorter than the penetration depth.

PA has successfully detected the 5 femto liter concentration of near IR dye in a whole body. The experiment consisted of imaging rat administered with indocyanine dye. After focusing the 532 nm pulsed laser (6.5 ns width, 10 MHz frequency), generated ultrasound was picked up by an array of ultrasound transducer. Constructed 3D image of the rat brain showed the dye flow dynamics. A similar strategy can track the drug-delivery particles functionalized with IR dyes [115].

6.3.2 Cell level study

A previous study showed that the 10 pM of anti-inflammatory drug-gold conjugate can be detected in 8 mm thick Rat joint with an SNR up to 17 times. Maximum spatial resolution of each image was limited to 250 μ m [116]. However, at shallower depth, single cell in circulation can be detected.

6.4 Spectroscopy

Recent development in CCD combined with confocal arrangement has improved sensitivity and resolution to match that of molecular imaging. Many optical spectroscopies including Raman microscopy [117], Fourier transformed infrared spectroscopy [118], photothermal spectroscopy [119] and ultrasound modulated optical tomography [120] have been used for imaging the drug release. However, Raman spectroscopy has potential due to its high multiplexing capabilities, high chemical specificity and non-susceptibility to photobleaching.

Raman spectroscopy detects the molecule by measuring change in scatter light. Frequency shift is the result of influence on light caused by vibrating molecules. Because shift is dependent on the charge and size of molecules, each molecule can be detected with high specificity [121]. Combining this spectroscopy with confocal arrangement, 1 μ m spatial resolution is achieved [122].

For drug-release study, a signal from drug molecule must be differentiated from the molecules present in background. For example, sulphathiazole release from the polymer microparticles into glycerol medium was quantified by acquiring spectrum for drug (sulphathiazole salt), polymethylsilsequioxane (particle) and glycerol-drug composite as shown in Figure 1B. Peaks corresponding to drug were identified in the spectrum of glycerol-drug mixture of varying concentration (Figure 1A). Subsequently, Raman images of sulphathiazole release from particle were acquired. The drug concentration was measured by following the drug peaks identified earlier. As shown in Figure 2, each pixel contains the circled peaks from the spectrum (Figure 1B) related to particular molecule (red for glycerol, black for the sulphathiazole drug) and intensity of those

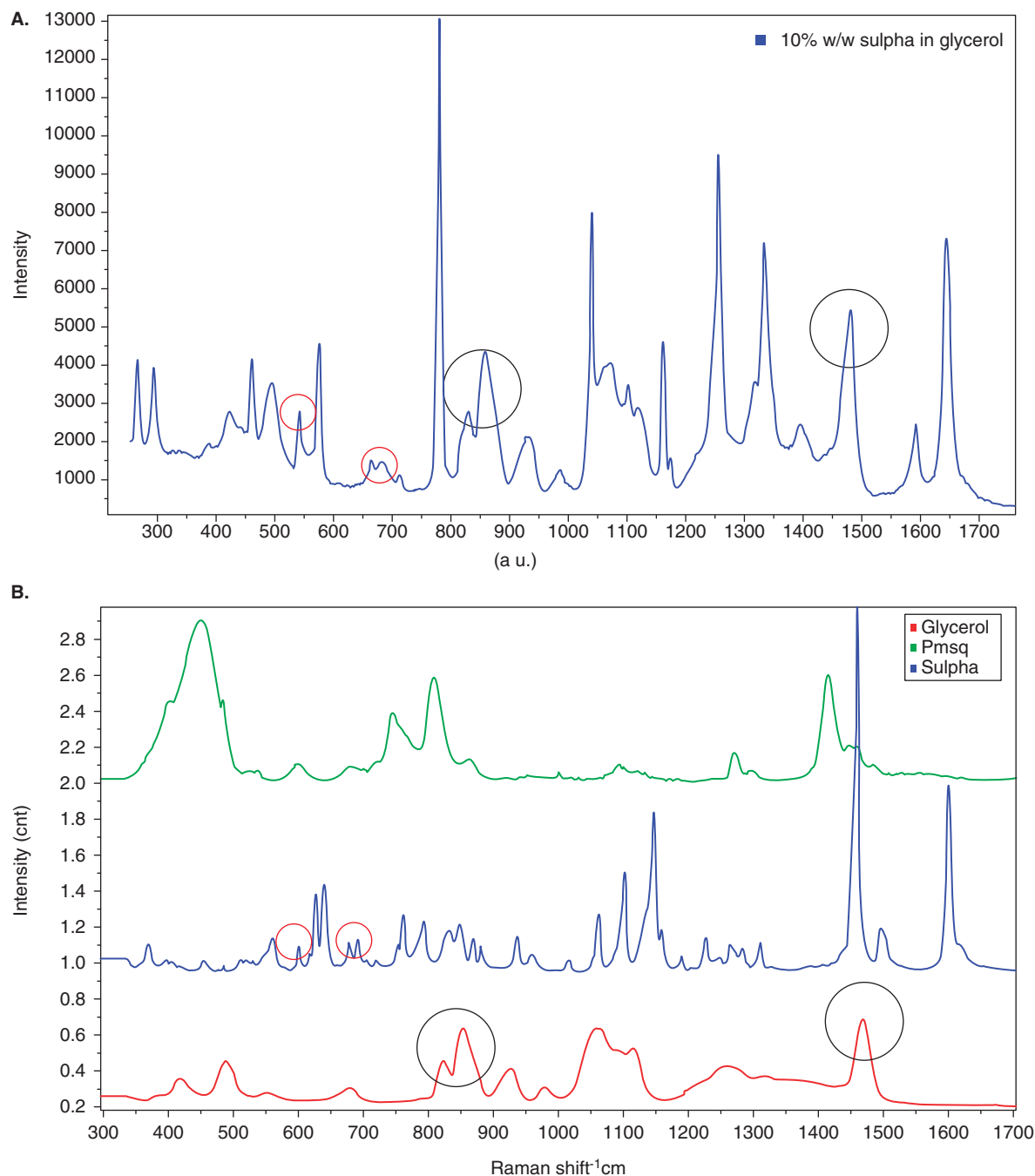


Figure 1. (A) shows the Raman spectrum of a sulfathiazole salt infused glycerol. Spectrum (A) was acquired in the vicinity of PMSQ microparticles where sulfathiazole salt was releasing from polymeric particle into the matrix of glycerol. Figure 1 (B) shows the Individual Raman spectrum of PMSQ, sulfathiazole salt and glycerol. The peaks in (B) with black circles refer to glycerol and peaks with red circle refer to sulphathiazole appear in the spectrum (A). This correlation between peaks in an individual spectrum (B) and spectrum of drug infused glycerol (A) confirms the release of sulfathiazole into the glycerol matrix surrounding a polymer particle.

PMSQ: Polymethylsilsesquioxane.

pixels determined the concentration of particular molecule. Temporal series of false color images showed the variation in concentration of solute, solution and solvent. Spatio-temporal correlation to these images ascertains the diffusion coefficient [123].

6.4.1 Whole body study

Typical tissue spectrum contains narrow spectral of Raman sensitive molecules allowing easy differentiation from the autofluorescence. A contribution of these molecules to total spectrum is proportionate to its abundance in tissue and,

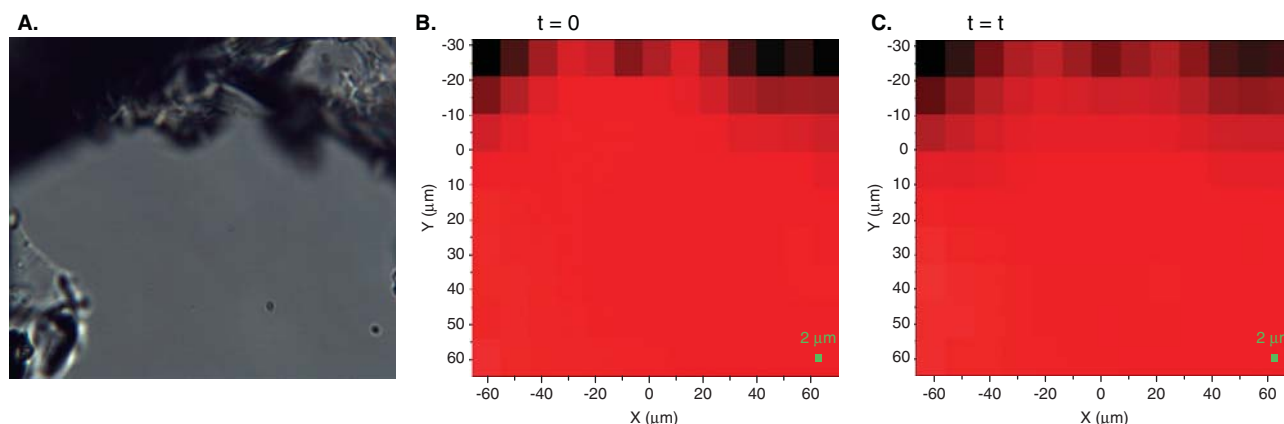


Figure 2. Shows false color Raman microscope images depicting temporal release of sulfathiazole from the particle into surrounding glycerol matrix. Red color represents pure glycerol whereas black color represents the sulfthiazole drug molecules. (A) Microscope image showing glycerol-particle interface. (B and C) Raman microscope image showing diffusion of sulfathiazole salt into glycerol matrix. Direction of diffusion is in downward direction of image.

thus, the rigorous quantification of drug release is possible. However, the inherent weak nature of the Raman signals restricts the sensitivity for *in vivo* studies [124].

The phenomenon called surface enhancement Raman scattering (SERS) amplifies the weak signals. A SERS occurs when electromagnetic field generated on the surface of gold nano-particles excites the surrounding molecules resulting in stronger signals [125]. SERS facilitated determining silica shelled gold nano-particles concentration in rat liver. Similarly, it has also confirmed the inability of pegylation on kinetics of the nano-particles in rat body. The experiment demonstrated high sensitivity by detecting 250 fmol of the pegylated and nonpegylated particles in 260 ml volume [126].

6.4.2 Cell level study

Uptake of deuterated liposomes was quantified and compared with the uptake of TAT (transactivation of transcription) peptide-modified liposomes. By determining signal amplitude ratio of C-D stretch (liposome) to C-H stretch (cell), the uptake of the liposome was resolved. High chemical specificity clearly showed the higher uptake of modified liposome [127].

6.5 Coherent anti-stoke Raman spectroscopy

Coherent anti-stoke Raman spectroscopy (CARS) is a probe-free, high resolution, non-invasive imaging technique that allows real-time imaging of bio-processes. The method has been used in disease detection, single cell study and biomedical imaging due to its capability to generate directional high amplitude signals of narrow bandwidth [128].

6.6 Whole body study

Because it is sensitive to various vibration modes of chemical bonds, images are constructed by following the bonds such as -OH in water, -CH in organic molecules and -PO bonds

in cellular molecules. In particular, lipid is used as a contrast molecule for imaging the biological system. However, because of limited depth resolution (100 μm and 5 mm with small objective lens) sub-surface details can only be captured. One good example is imaging of minimally excised rat spinal cord by following $-\text{CH}_2$ bond vibration [129]. Because higher depth resolution can be achieved via pumping more energy through laser, the fiber optical parametric oscillator is used to match phase with tight focusing. Similarly, the sciatic nerve of the rat was visualized with minimal intervention. The strong signals from the lipid rich white matter in CNS give rise to high contrast and allow capturing cellular details while imaging the entire organ. High strength of signals from lipid droplet aids in tracking their fast movement [130].

6.6.1 Cell level study

CARS has demonstrated subcellular resolution capability in observing the uptake of unlabeled nano-particles. To identify the nano-particles (PLGA), pump and stokes laser were tuned to 14,140 and 11,300 cm^{-1} respectively. The probe, pump and stoke beams interact to generate anti-stoke field. Because molecular vibration mode and molecule type affect the anti-stokes field, PLGA signature in cell can be identified [131]. This chemical selective strategy can also capture the image of the skin, sebaceous and adipocytes glands in the mouse. Tuning system to different vibration stretch, mineral oil diffusion in the skin can be obtained. With such techniques, 29 μM of concentration with 0.3 μm lateral and 0.9 μm depth resolution can be detected [132].

6.6.2 Other spectroscopy

This section briefly discusses the application of mass spectroscopy. The distribution of moxifloxacin in tuberculosis infected rabbit lungs was studied using mass spectroscopy. The study consisted of imaging 12 mm thick lung section

after administering 25 µg drug orally to the rabbit. First, 10 µg/ml of low-molecular mass compound in the form of matrix was applied to absorb extra laser energy without degrading ions emitting from the sample. Each slice is then fixated, washed and digested before scanning with pulsed laser beam [133]. Generated ions were sent to mass analyzer for obtaining their distribution on surface. Silver, gold and iron oxide layers on sample can increase the sensitivity to detect fatty acids, phospholipids and glycopospholipids [134].

Conventionally, these images are validated using whole body autoradioluminography. Validation identifies molecular signals concealed in tissue background [135] but sensitivity for large molecules improves significantly in the secondary ion system [136].

7. Hybrid imaging

A concept behind this is to combine the complementary imaging modalities to accrue greater benefits. Hybrid PET/CT successfully detected microphage in atherosclerotic plaque using trimodal nano-particles of copper radioisotope. Images of the mice administered with ⁶⁴Cu functionalized particles showed the accumulation of the particles in aortic root and arch. Conversely, CT captured the detailed image of murine vasculature. Hybrid approach has successfully demonstrated the combination of high sensitivity (0.1 µg/ml) with anatomical details to generate a precise map of nano-particle uptake in atherosclerotic vascular territories [137].

Many other methods of hybridization such as PET/optical, MRI/PET and MRI/optical are proposed [138]. MRI/PET can provide the spatial and functional data simultaneously but it reduces the investigation time for animal. Combining functional MRI such as perfusion and receptor binding to PET quantification has the potential to image real-time drug concentration and its cellular effect [139]. Attaching biomolecules to nano-particles or microbubbles can result in a multimodal contrast agent capable of imaging the same target at multiple length scale. Multimodal agents such as ultrasound/PET [140], PET/MRI [141] and magneto-fluorescent [142] are already in use. For example, RGD functionalized quantum dots with paramagnetic coating detected their internalization and expression of integrins while MRI can visualize through opaque tissue [143]. This approach detects inflammation [144], atherosclerosis [145] and apoptosis [146] using various ligands. Combining PA with Raman spectroscopy in infrared region enhances chemical specificity and, hence, it can quantify the topical availability of drug via spectral depth profiling. Such a hybrid approach improves the depth resolution by 2 – 3 times in comparison to OCT system while maintaining < 200 µm spatial resolution [147].

8. Expert opinion

Collecting data as image will emerge as a favorite form due to its statistically relevant 3D format and its ability to capture

spatio-temporal changes in drug concentration. However, it must allow correlation of data across length and time scale to preserve efforts in developing drug delivery and potentially bridging gap between preclinical and clinical trials. Further improvement in data acquisition speed, data analysis techniques and economic advantages may allow applying combinatorial approach to screen favorable carrier material-drug conjugation. Molecular resolution of imaging methods will permit capturing molecular events at a cell level following the drug dosing. Many methods such as mass spectroscopy, micro focus X-ray and secondary ion spectroscopy can provide such information *in vitro* and will continue to provide crucial data. However, requirement of sample preparation and use of high energy will limit its *in vivo* application.

Besides micro scale information, macro level information is also crucial for validating the DDS in clinical environment. Methods such as X-ray, magnetic resonance and radionuclide-based imaging will remain core to drug delivery characterization because of their clinically relevant spatial and depth resolution. PET/SPECT is considered the gold standard for quantifying the drug release due to high SNR. However, their temporal resolution and multiplexing capability need further development. Using high dose of short-life radioactive marker, the temporal resolution of PET is improved. However, there is a scope for further improvement. Importantly, radio-markers must be prepared in proximity of the imaging suit. In case of SPECT, its collimator design must be improved further. Recent addition of many radiopharmaceutical products capable of attaching to specific molecules has allowed multiplexing. Nevertheless, more of such discovery is required for multiplexing.

In MRI, overdependence on nitrogen oxide-based compound can restrict its use as a drug delivery research tool. However, bench-top MRI can be a useful tool in drug delivery research. Applying relaxometry to bench-top model, most *in vitro* and small animal studies can be carried out with reasonable resolution. Because of low signal intensity, long acquisition time and possibility of artefacts, a novel range of MRI probes are required for further development. A super cooled array of the detector combined with high magnitude magnetic field generating technology can improve speed and sensitivity of the system. Contrast molecule development will remain central to imaging in drug delivery. The concern of its influence over drug diffusion has to be studied further and an appropriate validating model will soon come out. The major challenge will be to extract more information out of the resonance phenomenon as it will achieve acquisition of the fastest drug-release data at molecular resolution acquisition.

Despite the noticeable progress in imaging, the difference of pharmacodynamics obtained via various imaging modalities (barring few) cannot be verified in the absence of an established validating method. Establishing a model to predict optical signal absorption/diffraction in biological tissue is vital for quantifying *in vivo* drug release. Recently developed models have resulted in the designing of the lens capable of correcting the diffracted signals. Such models will improve

depth resolution and accuracy of drug quantification. At present, collecting data near to drug release using endoscope will be used for *in vivo* studies. The endoscopy using Raman or CARS spectroscopy offers a new paradigm of detecting 3D picture of drug distribution with minimal invasion. Further development of such modalities in other disease models will be welcome due to their high chemical specificity. A new contrast agent for nonlinear microscopy combined with ultrafast laser source is required for further enhancement in the capability of optical system. A tag free imaging is preferred to limit the influence of dye molecule on drug diffusion. Spectroscopy can detect chemical with high specificity and sensitivity. However, their weak signals and low SNR require attention. Increasing brightness of the light source capable of tunability can increase SNR. Combining ultrasound-optical and Raman-optical coherence can improve the depth resolution and SNR. Specifically, nano-structured SERS imaging agents capable of attaching to drug molecule will be an important strategy in drug delivery studies.

Development in contrast molecule will be important in increasing efficiency of imaging modality. Many bio-markers capable of providing high contrast images are emerging, for example, hemoglobin and deoxyhemoglobin in breast model. Research progress in finding novel endogenous/exogenous contrast agents (high absorbing/emitting NIR dye and quantum dots) will remain critical. Although luciferase assisted optical tomography has improved the depth resolution, its use in brain studies may be difficult due to natural barrier. Transfection may allow drug molecule but entry of fluorescent protein remains doubtful. Moreover, the intensity of fluorescent signal must be kept constant to quantify the drug amount.

Hybrid imaging has a potential to provide the desired imaging system. Currently, a data fusion technique will continue to be applied for multimodal imaging. However, a seamless physical combination of complementary imaging method is essential to reap benefits. Initial investment, reluctance of commercial player and cost factor often limit development in this field. Moreover, technological hurdles such

as adaptation of signal detector to operate in the physical environment of other imaging modalities must be overcome. New combinations such as optical/MRI, optical/PET and PET/MRI may offer a combination of functional, structural and molecular imaging. Additionally, one type of energy may help another imaging modality as in the case of laser-induced hyperpolarization of molecule that provides MRI contrast to molecules. Development of a new generation of contrast agents capable of generating contrast for dual modality should continue. The PA method will find routine use in assessing drug response in organs, due to its multiscale imaging capability. Presence of bones limits the application of PA. However, if a universal method of phase shifting correction is developed, PA can find wider use in clinical set up. Moreover, this hybrid imaging can be interfaced with disease treatment and the drug dosing.

Rapid pace of improvement in imaging technologies will eventually replace the clinical trials in future. For future development, the use of nano-photonics can be extended into macro scale using an array of photonics structure. Nano-photonics has a capacity to overcome the diffraction limit. Even smaller fluid units acting as photonics can be administered intravenously to obtain high amplitude signals. New classes of metamaterial lenses (superlens) and nanolenses have raised the hope for a high and adaptable depth resolution. Similarly, it has been recently observed that the high frequency wave (X-ray region) without ionizing effect can be generated from the carbon nanotubes. This can potentially be used to obtain high contrast images without the side effects of ionization. Finally, it is worth noting that the interactions of optical waves and very high frequency ultrasound or magnetic field have the potential to provide super resolutions.

Declaration of interest

The author declares no conflict of interest. The work is part of funding provided by the IDEAS institute, The Robert Gordon University.

Bibliography

Papers of special note have been highlighted as either of interest (●) or of considerable interest (●●) to readers.

1. Brannon-Peppas L, Blanchette JO. Nanoparticle and targeted systems for cancer therapy. *Adv Drug Deliv Rev* 2004;9(11):1649-59
- **Comprehensive review on nano-particle-based drug delivery system.**
2. Damle NK, Frost P. Antibody-targeted chemotherapy with immunoconjugates of calicheamicin. *Curr Opin Pharmacol* 2003;3:386-90
3. Milenic DE, Brady ED, Brechbiel MW. Antibody-targeted radiation cancer therapy. *Nat Rev Drug Discov* 2004;3:488-98
4. Allen TM. Ligand-targeted therapeutics in anticancer therapy. *Nat Rev Drug Discov* 2002;2:750-63
5. Torchilin VP. Recent advances with liposomes as pharmaceutical carriers. *Nat Rev Drug Discov* 2005;4:145-60
- **Provides overview of liposomal drug carriers and its advantages and disadvantages.**
6. O'Shaughnessy JA, Blum JL, Sandbach JF, et al. Weekly nanoparticle albumin paclitaxel (Abraxane) results in long-term disease control in patients with taxane-refractory metastatic breast cancer. *Breast Cancer Res Treat* 2004;88:S65
7. Allison SD. Analysis of initial burst in PLGA microparticles. *Expert Opin Drug Deliv* 2008;5(6):615-28
- **A method of analyzing initial burst release from particles.**
8. David A, Kopeckova P, Minko T, et al. Design of a multivalent galactoside ligand for selective targeting of HPMA copolymer-doxorubicin conjugates to human colon cancer cells. *Eur J Cancer* 2004;40(1):148-57
9. Siepmann J, Lecomte F, Bodmeier R. Diffusion-controlled drug delivery systems: calculation of the required composition to achieve desired release profiles. *J Control Release* 1999;60(2-3):379-89
- **A comprehensive review of mathematic model to calculate release rate.**
10. Mahato RI. Water insoluble and soluble lipids for gene delivery. *Adv Drug Deliv Rev* 2005;57(5):699-712
11. Mader K, Bittner B, Li Y, et al. Monitoring microviscosity and microacidity of the albumin microenvironment inside degrading microparticles from poly(lactide-co-glycolide) (PLG) or ABA-triblock polymers containing hydrophobic poly (lactide-co-glycolide) a blocks and hydrophilic poly(ethyleneoxide) b blocks. *Pharm Res* 1998;15(5):787-93
- **Use of EPR imaging for measuring physical properties of microenvironment.**
12. Li LC. In vitro controlled release of theophylline from tablets containing a silicone elastomer latex. *Int J Pharm* 1992;87(1-3):117-24
13. Colombo P, Bettini R, Peppas NA. Observation of swelling process and diffusion front position during swelling in hydroxypropyl methyl cellulose (HPMC) matrices containing a soluble drug. *J Control Release* 1999;61(1-2):83-91
14. Nimai D, Salepkar A. Controlled release composition for active substances in an aqueous medium, International publication number. WO9414479; 1994
15. Mader K. Non-invasive spectroscopic and imaging techniques in drug delivery. *Adv Drug Deliv Rev* 2005;57(8):1083-4
- **General overview on the all non-invasive imaging techniques in the context of drug delivery.**
16. Ong J, Jennings R, Rhodes C, et al. Transmucosal delivery of peptides and proteins. US20090291886A1; 2009
17. Pitt WG, Hussein GA, Staples BJ. Ultrasonic drug delivery—a general review. *Expert Opin Drug Deliv* 2004;1(1):37-56
18. Dujardin N, Staes E, Kalia Y, et al. In vivo assessment of skin electroporation using square wave pulses. *J Control Release* 2002;79(1-3):219-27
19. Uhrich KE, Cannizzaro SM, Langer RS, et al. Polymeric systems for controlled drug release. *Chem Rev* 1999;99(11):3181-98
20. Bhavsar MD, Amiji MM. Polymeric nano- and microparticle technologies for oral gene delivery. *Expert Opin Drug Deliv* 2007;4(3):197-213
21. O'Riordan CR, Lachapelle A, Delgado C, et al. PEGylation of adenovirus with retention of infectivity and protection from neutralizing antibody in vitro and in vivo. *Hum Gene Ther* 1999;10(8):1349-58
22. Li LC, Deng J, Stephens D. Polyanhydride implant for antibiotic delivery—from the bench to the clinic. *Adv Drug Deliv Rev* 2002;54(7):963-86
23. Jain NK, Asthana A. Dendritic systems in drug delivery applications. *Expert Opin Drug Deliv* 2007;4(5):495-512
24. Majumdar S, Mitra AK. Chemical modification and formulation approaches to elevated drug transport across cell membranes. *Expert Opin Drug Deliv* 2006;3(4):511-27
25. Junginger HE, Hoogstraate JA, Verhoef JC. Recent advances in buccal drug delivery and absorption—in vitro and in vivo studies. *J Control Release* 1999;62(1-2):149-59
26. Gomez-Gaete C, Tsapis N, Besnard M, et al. Encapsulation of dexamethasone into biodegradable polymeric nanoparticles. *Int J Pharm* 2007;331(2):153-9
27. Allen TM, Cullis PR. Drug delivery systems: entering the mainstream. *Science* 2004;303:1818-22
28. Persson NO, Lindblom G, Bogentoft C, et al. NMR diffusion measurement in polymeric membranes used for controlled drug release. *Acta Pharm Suec* 1981;18(1):35-44
29. Dinarvand R, Wood B, D'Emanuele A. Measurement of the diffusion of 2,2,2-trifluoroacetamide within thermoresponsive hydrogels using NMR imaging. *Pharm Res* 1995;12(9):1376-9
30. Merchant FJ, Margaritis A, Wallace JB, et al. Novel technique for measuring solute diffusivities in entrapment matrices used in immobilization. *Biotechnol Bioeng* 1987;30(8):936-45
31. Campbell RD. Vital marking of single cells in developing tissues: india ink injection to trace tissue movements in hydra. *J Cell Set* 1973;13:651-66
32. Pancholi K, Stride E, Edirisinghe M. In vitro method to characterize diffusion of dye from polymeric particles: a model for drug release. *Langmuir* 2009;25(17):10007-13
33. Karmali PP, Simberg D. Interactions of nanoparticles with plasma proteins:

- implication on clearance and toxicity of drug delivery systems. *Expert Opin Drug Deliv* 2011;8:343-57
34. Ren T, Zhang J, Plachez C, et al. Diffusion tensor magnetic resonance imaging and tract-tracing analysis of probst bundle structure in Netrin1- and DCC-Deficient Mice. *J Neurosci* 2007;27(39):10345-9
 35. Swartz H. Seeing is believing—visualizing drug delivery in vitro and in vivo. *Adv Drug Deliv Rev* 2005;57:1085-6
 - **A short commentary on the concept of visualization of drug release from nano-particles using imaging system.**
 36. Lombry C, Dujardin N, Preat V. Transdermal delivery of macromolecules using skin. *Electroporation. Pharma Res* 2000;17(1):32-7
 37. Ho L, Cuppok Y, Muschert S, et al. Effects of film coating thickness and drug layer uniformity on in vitro drug release from sustained-release coated pellets: a case study using terahertz pulsed imaging. *Int J Pharm* 2009;382(1-2):151-9
 38. Colombo P, Bettini R, Santi P, et al. Swellable matrices for controlled drug delivery: gel-layer behaviour, mechanisms and optimal performance. *Pharm Sci Technol Today* 2000;3(6):198-204
 - **Describes the importance of the drug-release visualization and its importance in optimizing release.**
 39. Sitterberg J, Ozcetin A, Ehrhardt C, et al. Utilising atomic force microscopy for the characterisation of nanoscale drug delivery systems. *Eur J Pharm Biopharm* 2010;74(1):2-13
 - **A comprehensive review on characterization of drug delivery at nano-scale using AFM and its importance in understanding the carrier design.**
 40. Chithrani BD, Ghazani AA, Chan WC. Determining the size and shape dependence of gold nanoparticle uptake into mammalian cells. *Nano Lett* 2006;6(4):662-8
 41. Connor EE, Mwamuka J, Gole A, et al. Gold nanoparticles are taken up by human cells but do not cause acute cytotoxicity. *Small* 2005;1:325-7
 42. Tardif JC, Lesage F, Harel F. Imaging biomarkers in atherosclerosis trials. *Circ Cardiovasc Imaging* 2011;4(3):319-33
 43. Lu ZR. Molecular imaging of HPMa copolymers: Visualizing drug delivery in cell, mouse and man. *Adv Drug Deliv Rev* 2010;62(2):246-57
 - **Application of molecular imaging in assessing drug delivery in vivo.**
 44. Kherlopian AR, Song T, Duan Q, et al. A review of imaging techniques for systems biology. *BMC Syst Biol* 2008;2:74
 - **A review on molecular imaging in context of system biology including drug delivery and development.**
 45. Pancholi K, Edirisinghe M, Stride E. Spatio-temporal image correlation analysis of ultrasound mediated diffusion. 2010; (unpublished)
 46. Massoud TF, Gambhir SS. Molecular imaging in living subjects: seeing fundamental biological processes in a new light. *Genes Dev* 2003;17(5):545-80
 - **An excellent review on imaging systems from considering biology in clinical and laboratory points of view.**
 47. Cernea S, Kidron M, Wohlgelernter J, et al. Comparison of pharmacokinetic and pharmacodynamic properties of single-dose oral insulin spray and subcutaneous insulin injection in healthy subjects using the euglycemic clamp technique. *Clin Ther* 2004;26(12):2084-91
 48. Marra M, Gukasyan HJ, Raghava S, et al. 2nd Ophthalmic drug development and delivery summit. *Expert Opin Drug Deliv* 2007;4(1):77-85
 49. Krishnaiah YS, Satyanarayana S, Rama Prasad YV, et al. Gamma scintigraphic studies on guar gum matrix tablets for colonic drug delivery in healthy human volunteers. *J Control Release* 1998;55(2-3):245-52
 50. Herkenne C, Alberti I, Naik A, et al. In vivo methods for the assessment of topical drug bioavailability. *Pharm Res* 2008;25(1):87-103
 51. Faiyazuddin MD, Ahmad S, Mustafa G, et al. Bioanalytical approaches, bioavailability assessment, and bioequivalence study for waiver drugs: in vivo and in vitro perspective. *Clin Res Regul Aff* 2010;27(2):32-41
 52. Morimoto K, Nagayasu A, Fukunoki S, et al. Evaluation of polyvinyl alcohol hydrogel as sustained-release vehicle for transdermal sytem of Bunitrolol-HCL. *Drug Dev Ind Pharm* 1990;16(1):13-29
 53. Surber C, Schwarb FP, Smith EW. Tape-stripping technique. *Cutan Ocul Toxicol* 2001;20(4):461-74
 54. Beger RD, Sun J, Schnackenberg LK. Metabolomics approaches for discovering biomarkers of drug-induced hepatotoxicity and nephrotoxicity. *Toxicol Appl Pharmacol* 2010;243(2):154-66
 55. McNamee CE, Pyo N, Higashitani K. Atomic force microscopy study of the specific adhesion between a colloid particle and a living melanoma cell: effect of the charge and the hydrophobicity of the particle surface. *Biophys J* 2006;91(5):1960-9
 56. Seddon BM, Workman P. The role of functional and molecular imaging in cancer drug discovery and development. *Br J Radiol* 2003;76:128-38
 - **Explains the importance of imaging in drug development overlaps with drug delivery.**
 57. Fu K, Pack DW, Klibanov AM, et al. Visual evidence of acidic environment within degrading poly(lactic-co-glycolic acid) (PLGA) microspheres. *Pharm Res* 2000;17(1):100-6
 - **Method of visualization of microenvironment.**
 58. Badkar AV, Smith AM, Eppstein JA, et al. Transdermal delivery of interferon alpha-2B using microporation and iontophoresis in hairless rats. *Pharm Res* 2007;24(7):1389-95
 59. Livingston J. Genetically engineered mice in drug development. *J Int Med* 1999;245(6):627-35
 60. Wilding IR, Coupe AJ, Davis SS. The role of gamma-scintigraphy in oral drug delivery. *Adv Drug Deliv Rev* 2001;46(1-3):103-24
 61. Newman SP. Scintigraphic assessment of therapeutic aerosols. *Crit Rev Ther Drug Carrier Syst* 1993;10(1):65-109
 62. Oyen WJ, Boerman OC, Storm G, et al. Detecting infection and inflammation with technetium-99m-labeled Stealth liposomes. *J Nucl Med* 1996;37(8):1392-7
 63. Allen TM, Everest JM. Effect of liposome size and drug release properties on pharmacokinetics of encapsulated drug in rats. *J Pharmacol Exp Ther* 1983;226(2):539-44
 - **Evidence of the effect of physical properties of carrier on phamacokinetics.**

64. Coutts-London C, Wright N, Mieso E, et al. The use of FT-IR imaging as an analytical tool for the characterization of drug delivery systems. *J Control Release* 2003;93(3):223-48
- **Example method of FTIR in characterizing drug delivery system.**
65. Nathan B. In vivo molecular imaging: the inside job. *Nat Methods* 2009;6:465-9
- **An extensive review on molecular imaging and methods involved.**
66. Grange C, Geninatti-Crich S, Esposito G, et al. Combined delivery and magnetic resonance imaging of neural cell adhesion molecule-targeted doxorubicin-containing liposomes in experimentally induced Kaposi's sarcoma. *Cancer Res* 2010;70(6):2180-90
67. Chrystyn H. Methods to determine lung distribution of inhaled drugs - could gamma scintigraphy be the gold standard? *Br J Clin Pharmacol* 2000;49(6):525-8
- **Discusses requirement of validating imaging results.**
68. Hornack JP Basic of MRI, 1996. Available from: <http://www.cis.rit.edu/htbooks/mri/inside.htm> [Accessed on 10 May 2010]
69. Port RE, Wolf W. Non invasive methods to study drug distribution. *Invest New Drugs* 2003;21:157-68
70. Madhu B, Hjartstam J, Soussi B. Studies of internal flow process in polymers by H-1 NMR spectroscopy at 500 MHz. *J Control Release* 1998;56:95-104
71. Sun C, Lee JS, Zhang M. Magnetic nanoparticles in MR imaging and drug delivery. *Adv Drug Deliv Rev* 2008;60(11):1252-65
72. Saito R, Bringas JR, McKnight TR, et al. Distribution of liposomes into brain and rat brain tumor models by convection-enhanced delivery monitored with magnetic resonance imaging. *Cancer Res* 2004;64(7):2572-9
73. Viglianti BL, Abraham SA, Micheli CR, et al. In vivo monitoring of tissue pharmacokinetics of liposome/drug using MRI: illustration of targeted delivery. *Magn Reson Med* 2004;51(6):1153-62
- **Use of contrast agent to visualize the distribution of liposome in small animal via MRI.**
74. Muller TB, Haraldseth O, Jones RA, et al. Perfusion and diffusion-weighted MR imaging for in vivo evaluation of treatment with U74389G in a rat stroke model. *Stroke* 1995;26(8):1453-8
- **Functional imaging using perfusion and diffusion weighted method.**
75. Kim H, Robinson MR, Lizak MJ. Controlled drug release from an ocular implant: an evaluation using dynamic three-dimensional magnetic resonance imaging. *Invest Ophthalmol Vis Sci* 2004;45(8):2722-31
76. Morawski AM, Winter PM, Crowder KC, et al. Targeted nanoparticles for quantitative imaging of sparse molecular epitopes with MRI. *Magn Reson Med* 2004;51(3):480-6
77. Newman SP, Wilding IR. Imaging techniques for assessing drug delivery in man. *Pharm Sci Technol Today* 1999;2(5):181-9
78. Youngho S. Quantification of SPECT and PET for drug development. *Curr Radiopharm* 2008;1:17-21
- **Discusses SPECT and PET technologies in terms of quantifying the drug in vivo.**
79. Lee Z, Berridge MS, Finlay WH, et al. Mapping PET-measured triamcinolone acetonide (TAA) aerosol distribution into deposition by airflow generation. *Int J Pharm* 2000;199(1):7-16
80. Yamamoto Y, de Silva R, Rhodes CG, et al. Noninvasive quantification of regional myocardial metabolic rate of oxygen by 15O2 inhalation and positron emission tomography. *Experimental validation. Circulation* 1996;94(4):808-16
81. Chrastina A, Valadon P, Massey KA, et al. Lung vascular targeting using antibody to aminopeptidase P: CT-SPECT imaging, biodistribution and pharmacokinetic analysis. *J Vasc Res* 2010;47(6):531-43
82. Weber DA, Ivanovic M, Franceschi D, et al. Pinhole SPECT: an approach to in vivo high resolution SPECT imaging in small laboratory animals. *J Nucl Med* 1994;35(2):342-8
- **New design of collimator is used to show the capability of high resolution SPECT.**
83. Cherry SR, Gambhir SS. Use of positron emission tomography in animal research. *ILAR J* 2001;42(3):219-32
84. Teo BK, Seo Y, Bacharach SL, et al. Partial-volume correction in PET: validation of an iterative postreconstruction method with phantom and patient data. *J Nucl Med* 2007;48(5):802-10
85. Brooks DJ. Positron emission tomography and single-photon emission computed tomography in central nervous system drug development. *Neuro Rx* 2005;2(2):226-36
86. Dolovich M, Labiris R. Imaging drug delivery and drug responses in the lung. *Proc Am Thorac Soc* 2004;1(4):329-37
- **Molecular imaging applied to drug release in respiratory system.**
87. Blank A, Freed JH, Kumar NP, Wang CH. Electron spin resonance microscopy applied to the study of controlled drug release. *J Control Release* 2006;111(1-2):174-84
88. Mader K, Cremmilleux Y, Domb A, et al. In vitro/in vivo comparison of drug release and polymer erosion from biodegradable P(FAD-SA) polyanhydrides—a noninvasive approach by the combined use of electron paramagnetic resonance spectroscopy and nuclear magnetic resonance imaging. *Pharm Res* 1997;14:820-6
89. Moll KP, Stosser R, Herrmann W, et al. In vivo ESR studies on subcutaneously injected multilamellar liposomes in living mice. *Pharm Res* 2004;21(11):2017-24
90. Lurie DJ, Mader K. Monitoring drug delivery processes by EPR and related techniques—principles and applications. *Adv Drug Deliv Rev* 2005;57(8):1171-90
- **Extensive review on EPR imaging to study drug delivery process.**
91. Mader K, Bacic G, Domb A, et al. Noninvasive in vivo monitoring of drug release and polymer erosion from biodegradable polymers by EPR spectroscopy and NMR imaging. *J Pharm Sci* 1997;86(1):126-34
92. Cal K, Zakowiecki D, Stefanowska J. Advanced tools for in vivo skin analysis. *Int J Dermatol* 2010;49(5):492-9
93. Peppas NA, Gurny R, Doelker E, et al. Modeling of drug diffusion through swellable polymeric systems. *J Membr Sci* 1980;7:241-53
94. Ntziachristos V. Going deeper than microscopy: the optical imaging frontier in biology. *Nat Methods* 2010;7:603-14
- **Physics point of view on depth resolution of optical imaging and methods to improve it.**

95. Fritjof H, Winfried D. Deep tissue two photon microscopy. *Nat Methods* 2005;2:932-40
96. van den Bergh BA, Vroom J, Gerritsen H, et al. Interactions of elastic and rigid vesicles with human skin in vitro: electron microscopy and two-photon excitation microscopy. *Biochim Biophys Acta* 1999;1461(1):155-73
97. Wong C, Stylianopoulos T, Cui J, et al. Multistage nanoparticle delivery system for deep penetration into tumor tissue. *Proc Natl Acad Sci USA* 2011;108(6):2426-31
98. Roberts MS, Roberts MJ, Robertson TA, et al. In vitro and in vivo imaging of xenobiotic transport in human skin and in the rat liver. *J Biophotonics* 2008;1(6):478-93
99. Delehanty JB, Boeneman K, Bradburne CE, et al. Quantum dots: a powerful tool for understanding the intricacies of nanoparticle-mediated drug delivery. *Expert Opin Drug Deliv* 2009;6(10):1091-112
100. Zhang J. The colourful journey of green fluorescent protein. *ACS Chem Biol* 2009;4(2):85-8
101. Szeto HH, Schiller PW, Zhao K, et al. Fluorescent dyes alter intracellular targeting and function of cell-penetrating tetrapeptides. *FASEB J* 2005;19(1):118-20
102. Wender PA, Goun EA, Jones LR, et al. Real-time analysis of uptake and bioactivatable cleavage of luciferin-transporter conjugates in transgenic reporter mice. *PNAS* 2007;104:10340-5
103. Ghosn MG, Sudheendran N, Wendt M, et al. Monitoring of glucose permeability in monkey skin in vivo using. *Optical coherence tomography. J Biophotonics* 2010;3(1-2):25-33
- **Application of OCT to measure glucose diffusion into skin.**
104. Schmitt JM. Optical coherence tomography (OCT): a review, selected topics in quantum electronics. *IEEE J* 1999;5(4):1205-121
105. Ghosn MG, Carbajal EF, Befrui NA, et al. Permeability of hyperosmotic agent in normal and atherosclerotic vascular tissues. *J Biomed Opt* 2008;13(1):010505
106. Larin KV, Tuchin VV. Functional imaging and assessment of the glucose diffusion rate in epithelial tissues in optical coherence tomography. *Quantum Electro* 2008;38(6):551-6
107. Ghosn MG, Tuchin VV, Larin KV. Nondestructive quantification of analyte diffusion in cornea and sclera using optical coherence tomography. *Invest Ophthalmol Vis Sci* 2007;48(6):2726-33
108. Huang D, Swanson EA, Lin CP, et al. Optical coherence tomography. *Science* 1991;254(5035):1178-81
- **A comprehensive review on OCT from physics point of view.**
109. Tearney GJ, Brezinski ME, Bouma BE, et al. In vivo endoscopic optical biopsy with optical coherence tomography. *Science* 1997;276(5321):2037-9
- **Endoscopic approach in imaging using OCT.**
110. Kim CS, Wilder-Smith P, Ahn YC, et al. Enhanced detection of early-stage oral cancer in vivo by optical coherence tomography using multimodal delivery of gold nanoparticles. *J Biomed Opt* 2009;14(3):034008
111. Haisch C. Quantitative analysis in medicine using photoacoustic tomography. *Anal Bioanal Chem* 2009;393(2):473-9
112. Kim C, Favazza C, Wang LV. In vivo photoacoustic tomography of chemicals: high-resolution functional and molecular optical imaging at new depths. *Chem Rev* 2010;110(5):2756-82
113. Wang LV. Prospects of photoacoustic tomography. *Med Phys* 2008;35(12):5758-67
- **A review on PA imaging.**
114. Sivaramakrishnan M, Maslov K, Zhang HF, et al. Limitations of quantitative photoacoustic measurements of blood oxygenation in small vessels. *Phys Med Biol* 2007;52(5):1349-61
- **Discusses issues with quantifying drug in tissue using PA imaging.**
115. Laufer J, Delpy D, Elwell C, et al. Quantitative spatially resolved measurement of tissue chromophore concentrations using photoacoustic spectroscopy: application to the measurement of blood oxygenation and haemoglobin concentration. *Phys Med Biol* 2007;52(1):141-68
116. Chamberland DL, Agarwal A, Kotov N, et al. Photoacoustic tomography of joints aided by an Etanercept-conjugated gold nanoparticle contrast agent—an ex vivo preliminary rat study. *Nanotechnology* 2008;19(9):95101-8
117. Freudiger CW, Min W, SaarBG, et al. Label-free biomedical imaging with high sensitivity by stimulated raman scattering microscopy. *Science* 2008;322(5909):1857-61
118. Kazarian SG, Andrew Chan KL. "Chemical Photography" of drug release. *Macromolecules* 2003;36(26):9866-72
- **An imaging approach to study drug release.**
119. Gotter B, Faubel W, Neubert RH. Photothermal imaging in 3D surface analysis of membrane drug delivery. *Eur J Pharm Biopharm* 2010;74:26-32
120. Lev A, Sfez B. In vivo demonstration of the ultrasound-modulated light technique. *J Opt Soc Am A Opt Image Sci Vis* 2003;20(12):2347-54
121. Wartewig S, Neubert RH. Pharmaceutical applications of Mid-IR and Raman spectroscopy. *Adv Drug Deliv Rev* 2005;57(8):1144-70
122. Mansour HM, Hickey AJ. Raman characterization and chemical imaging of biocolloidal self-assemblies, drug delivery systems, and pulmonary inhalation aerosols: a review. *AAPS PharmSciTech* 2007;8(4):99
123. Pancholi KP. Quantification of drug diffusion coefficient of microparticulate drug delivery system using Raman. *Microscopy* 2011;Unpublished data
124. Hanlon EB, Manoharan R, Koo TW, et al. Prospects for in vivo Raman spectroscopy. *Phys Med Biol* 2000;45(2):1-59
125. Baena JR, Lendl B. Raman spectroscopy in chemical bioanalysis. *Curr Opin Chem Biol* 2004;8(5):534-9
- **A good review on Raman to analyze chemical concentrations.**
126. Keren S, Zavaleta C, Cheng Z, et al. Noninvasive molecular imaging of small living subjects using Raman spectroscopy. *Proc Natl Acad Sci* 2008;105(15):5844-9
- **A method of imaging small animal using Raman.**
127. Gotter B, Faubel W, Neubert RH. Optical methods for measurements of skin penetration. *Skin Pharmacol Physiol* 2008;21(3):156-65

128. Ji-Xin C. Coherent anti-stokes raman scattering microscopy, *Appl spectrosc.* 2007;61(9):197-208
129. Evans CL, Xie XS. Coherent anti-stokes Raman scattering microscopy: chemical imaging for biology and medicine. *Annu Rev Anal Chem* 2008;1:883-909
130. Henry FP, Cote D, Randolph MA, et al. Real-time in vivo assessment of the nerve microenvironment with coherent anti-Stokes Raman scattering microscopy. *Plast Reconstr Surg* 2009;123(2):123S-30S
- **Shows improvement in temporal resolution of CARS to detect chemical analyte in microenvironment.**
131. Xu P, Gullotti E, Tong L, et al. Intracellular drug delivery by poly(lactic-co-glycolic acid) nanoparticles. *Mol Pharm* 2009;6(1):190-201
132. Pezacki JP, Blake JA, Danielson DC, et al. Chemical contrast for imaging living systems: molecular vibrations drive CARS microscopy. *Nat Chem Biol* 2011;7(3):137-45
133. Chughtai K, Heeren RM. Mass spectrometric imaging for biomedical tissue analysis. *Chem Rev* 2010;110(5):3237-77
- **An extensive review on mass spectrometric method.**
134. Zaima N, Hayasaka T, Goto-Inoue N, et al. Matrix-assisted laser desorption/ionization imaging mass spectrometry. *Int J Mol Sci* 2010;11:5040-55
135. Stoeckli M, Staab D, Schweitzer A. Compound and metabolite distribution measured by MALDI mass spectrometric imaging in whole-body tissue sections international. *J Mass Spectrom* 2007;260(2-3):195-202
136. Belu AM, Davies MC, Newton JM, et al. TOF-SIMS characterization and imaging of controlled-release drug delivery systems. *Anal Chem* 2000;72(22):5625-38
137. Nahrendorf M, Zhang H, Hembrador S, et al. Nanoparticle PET-CT imaging of macrophages in inflammatory atherosclerosis. *Circulation* 2008;117(3):379-87
138. Cherry SR. Multimodality imaging: beyond PET/CT and SPECT/CT. *Semin Nucl Med* 2009;39(5):348-53
- **Discusses hybrid imaging beyond existing commercially available combinations.**
139. Pichler BJ, Judenhofer MS, Wehr HF. PET/MRI hybrid imaging: devices and initial results. *Eur Radiol* 2008;18(6):1077-86
140. Tartis MS, Kruse DE, Zheng H, et al. Dynamic microPET imaging of ultrasound contrast agents and lipid delivery. *J Control Release* 2008;131(3):160-6
141. Cherry SR, Louie AY, Jacobs RE. The integration of positron emission tomography with magnetic resonance imaging. *Proc IEEE* 2008;96:416-38
142. Kamaly N, Kalber T, Ahmad A, et al. Bimodal paramagnetic and fluorescent liposomes for cellular and tumor magnetic resonance imaging. *Bioconjug Chem* 2008;19:118-29
143. Tsourkas A, Shinde-Patil VR, Kelly KA, et al. In vivo imaging of activated endothelium using an anti-VCAM-1 magnetooptical probe. *Bioconjug Chem* 2005;16(3):576-81
144. Mulder WJ, Strijkers GJ, Griffioen AW, et al. A liposomal system for contrast-enhanced magnetic resonance imaging of molecular targets. *Bioconjug Chem* 2004;15(4):799-806
145. Kelly KA, Allport JR, Tsourkas A, et al. Detection of vascular adhesion molecule-1 expression using a novel multimodal nanoparticle. *Circ Res* 2005;96(3):327-36
146. van Tilborg GA, Mulder WJ, Chin PT, et al. Annexin A5-conjugated quantum dots with a paramagnetic lipidic coating for the multimodal detection of apoptotic cells. *Bioconjug Chem* 2006;17(4):865-8
147. Yakovlev VV, Zhang HF, Noojin GD, et al. Stimulated Raman photoacoustic imaging. *Proc Natl Acad Sci USA* 2010;107(47):20335-9

Affiliation

Ketan Pancholi
The Robert Gordon University,
School of Engineering,
Clarke Building Schoolhill Aberdeen
Aberdeenshire, UK
Tel: +01224262319;
E-mail: ketan.pancholi@gmail.com